Supporting Information

Controllable ionic liquid-assisted electrochemical exfoliate carbon fibers for the green and large-scale preparation of functionalized graphene quantum dots endowed with multicolor emitting and size tunability

Yuting Yan[a], Henan Li[b], Qirui Wang[a], Hanping Mao*[a], Wang Kun*[a,b]

[a]Key Laboratory of Modern Agriculture Equipment and Technology, Institute of Agricultural Engineering, Jiangsu University, Zhenjiang, 212013, P.R. China

[b]School of Chemistry and Chemical Engineering, Jiangsu University, Zhenjiang, 212013, P. R. China.

∗Corresponding author. Tel.: +86 511 88791800; fax: +86 511 88791708.
E–mail address: wangkun@ujs.edu.cn; maohp@ujs.edu.cn

Fig. S1

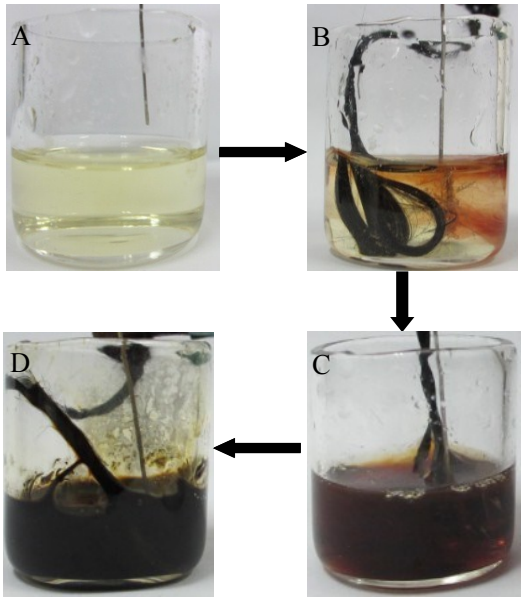

Fig. S1. Time evolution of ILs electrolyte and carbon fiber anode during exfoliation in [Bmim][BF_4] electrolyte in different stages (A: before exfoliation; B: the beginning of exfoliation; C: an hour in exfoliation; D: the end of exfoliation).

Quantum Yields (QYs) Measurements

The quantum yields of as-prepared G-GQDs were measured and calculated by using a comparative method (Table S1). Rhodamine B in water (QYs=0.31) was chosen as the standard fluorophore with excitation at 340 nm as the reference. And the quantum yields of the GQDs were calculated according to:

$$\Phi = \Phi_R \times \frac{I}{I_R} \times \frac{A_R}{A} \times \frac{n^2}{n_R{}^2}$$

Where Φ, I, n and A designates the quantum yield, measured integrated emission intensity, refractive index and the optical absorbance, respectively. The subscript "R" refers to standard with known quantum yield.

Table S1. QYs of the as-prepared G-GQDs

Sample	Integrated emissions intensity (*I*)	Abs. at 340 nm (*A*)	Refractive index of solvent (*n*)	Quantum yield (*Φ*)
Rhodamine B	19568	0.017	1.33	0.31 (known)
G-GQDs	13412	0.042	1.33	0.086

In addition, with the assistance of ionic liquid, G-GQDs with a quantum yield up to 8.6% are successfully prepared via electrochemical exfoliate, which is higher than that of the hydrothermal cleaving routes (< 8%).[1,2]

Characterization of the CFs

Raman spectroscopy is considered to be a powerful and efficient technique for characterizing the carbonization and graphitization on carbon-based materials.[3] The D- and G-band (I_D/I_G) ratio of Raman spectra is a parameter to estimate the disorder degree and the sp^2 domains. Thus, the Raman spectrum of starting material (CFs) as showed in Fig. S2A. The characteristic peaks at around 1359 cm^{-1} (D-band) and 1589 cm^{-1} (G-band), corresponding to the sp^3 hybridized and the sp^2 hybridized, respectively. Form the Raman spectra, it was observed that the small domain structure of the sp^2 in original CFs (Integrated intensity), which is beneficial to get size controlled synthesis of GQDs in accordance with Peng's report.[4] Meanwhile, the higher ratio of I_D/I_G (Integrated intensity) on original CFs indicated that the existence of non-graphitized structure in original CFs.[5,6]

Further, XRD tool was employed to study the crystalline structure of the original CFs presented in Fig. S2B. There is an obvious diffraction peak at ~25.0° can be observed in the spectrum, corresponding to the (002) diffraction of graphitic structures, the absence of the (110) band at ~44.0° even indicates a non-graphitized carbonaceous structure in original CFs.[7]

Combined with the analysis of Raman and XRD, it is clearly confirmed that CFs were possessed with carbonized structure. Such a carbonized CFs can be easily broken down, leading to the creation of GQDs with different size distribution in scalable amounts.

1 **Fig. S2**

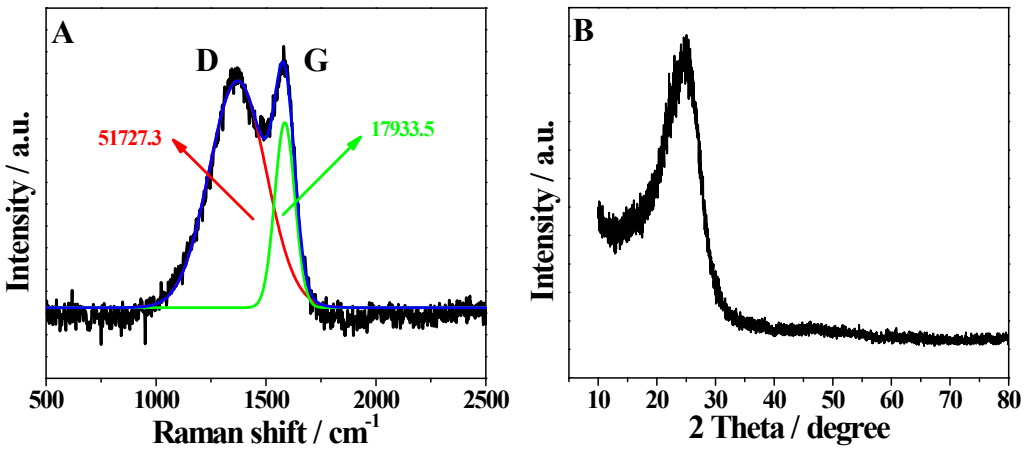

2

3 **Fig. S2**. Raman spectra (A) and XRD pattern (B) of original CFs.

Fig. S3

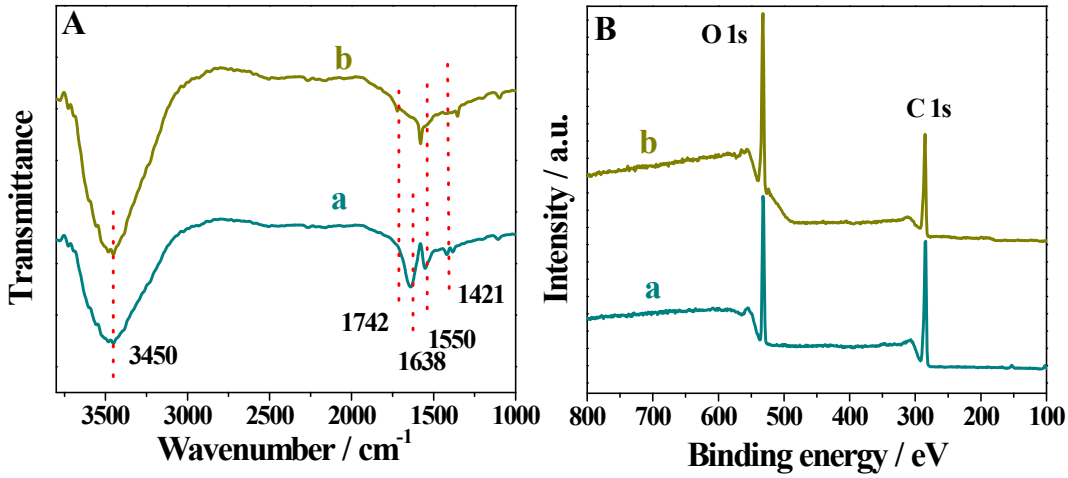

Fig. S3. (A) FTIR and (B) XPS spectra of G-GQDs (a) and Y-GQDs (b) were synthesized with ratios of H_2O/ILs at 15% and 30% as electrolyte, respectively.

Fig. S4

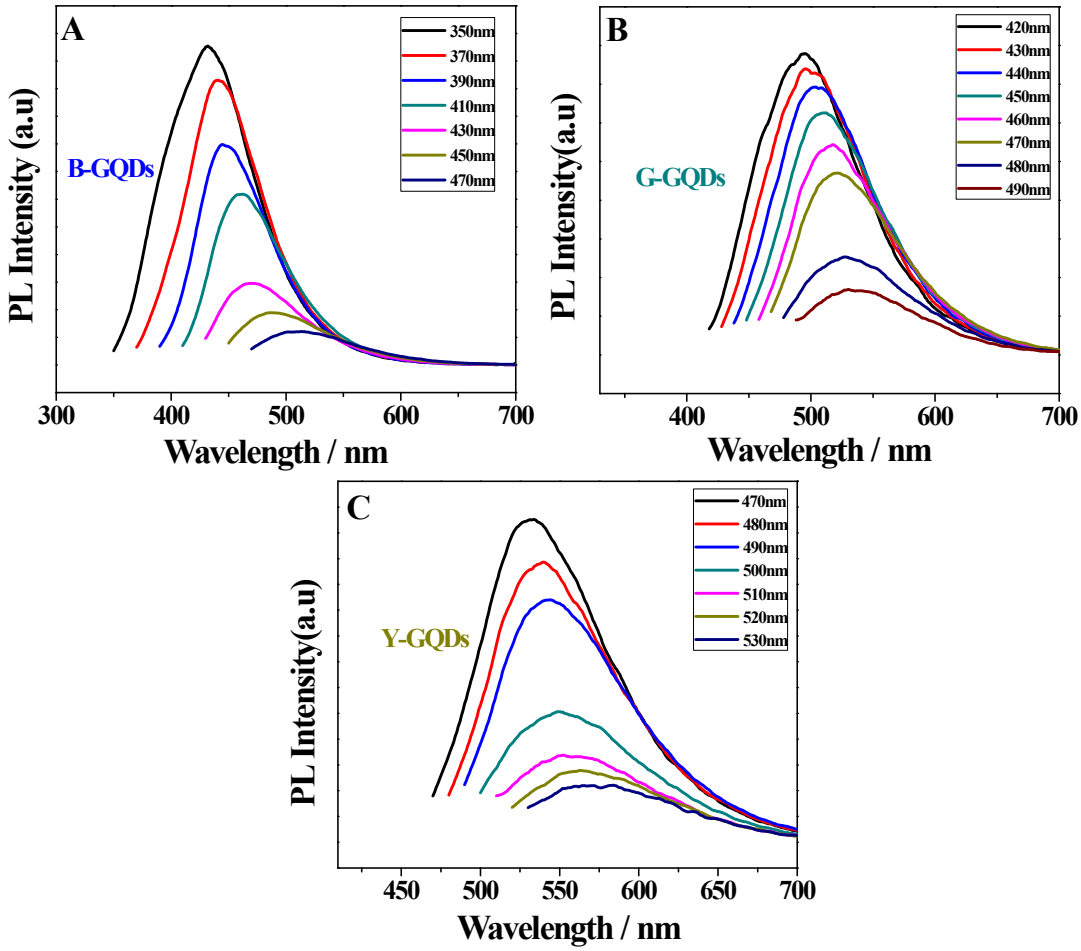

Fig. S4. The PL spectra of the (A) B-GQDs, (B) G-GQDs and (C) Y-GQDs aqueous solution excited by various wavelengths, respectively.

The effect of the water on the electrochemical properties of ILs

In order to investigate the influence of the water on the electrochemical properties of ILs, the cyclic voltammetrys (CVs) recorded in ILs contain different content of H_2O, as shown in Fig. S5. It is seen that the electrochemical potential window of the IL/water was decreased with the content of water from 0 vt % H_2O to 30 vt % H_2O (Fig. S5A). Thus, we can infer that the trend of decreasing activation voltages with increasing water content is correlated to the smaller over potential required for the electrochemical oxidation of water. As such, hydroxyl radicals released from the oxidation of water may play an important role. Meanwhile, the viscosity of ILs may be changed by other means such as stirring, so we also investigate the effect of stirring on viscosity of ILs by CV test. However, there is no any change on electrochemical potential window of pure ILs before and after stirring from CV curves (Fig. S5B).

Fig. S5

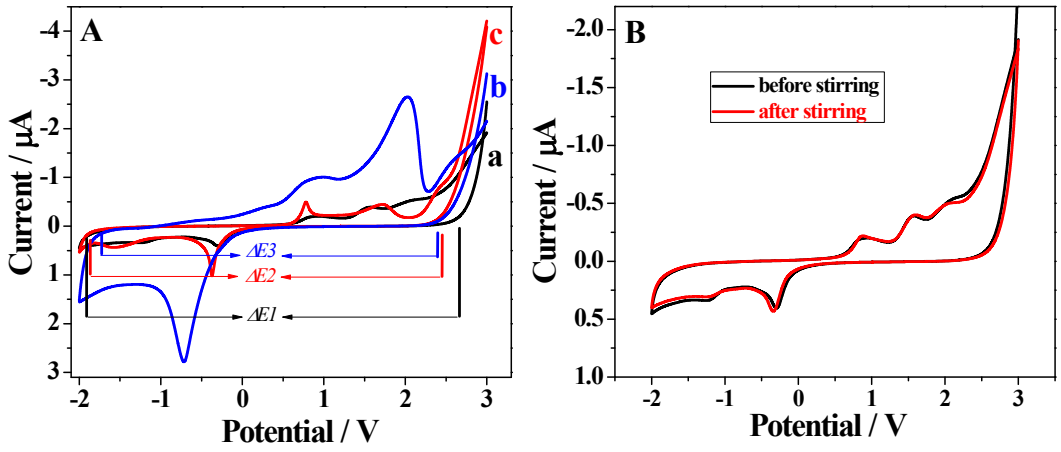

Fig. S5. (A) CVs curve recorded in different electrolyte with volume ratio of H_2O/ILs at (a) 0%, (b) 15% and (c) 30%, respectively; (B) CVs curve recorded in pure ILs before and after stirring.

Fig. S6

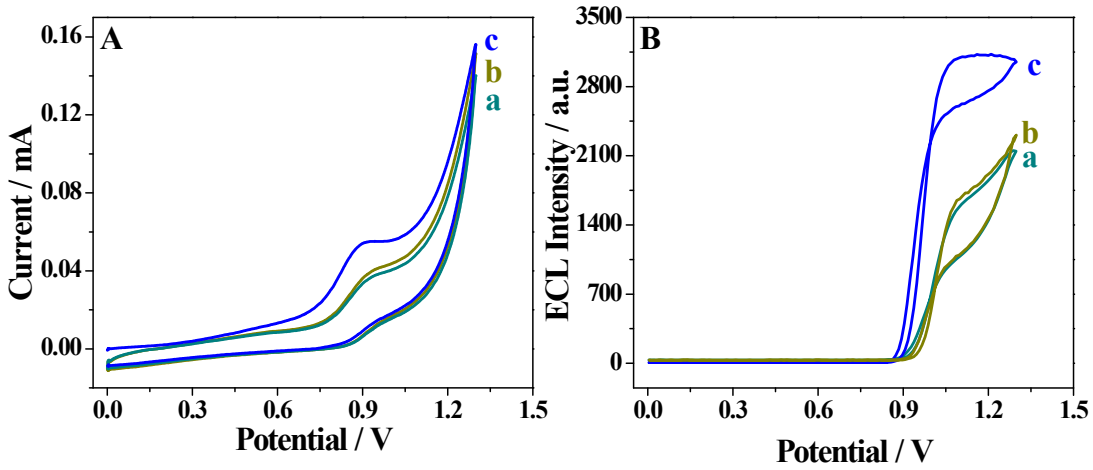

Fig. S6. (A) CV and (B) ECL-potential curves of (a) G-GQDs/Ru(bpy)$_3^{2+}$, (b) G-GQDs/Ru(bpy)$_3^{2+}$ and (c) B-GQDs/ Ru(bpy)$_3^{2+}$ in 0.1 M pH 9.0 PBS.

Fig. S7

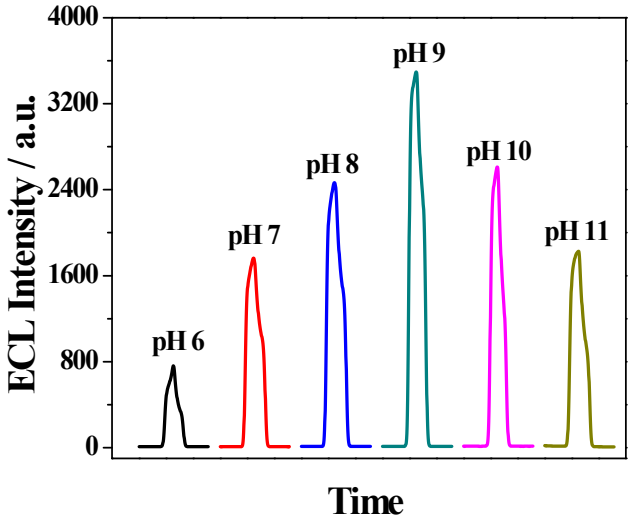

Fig. S7. ECL-potential curves of the B-GQDs/$Ru(bpy)_3^{2+}$ in PBS with different pH values.

Fig. S8

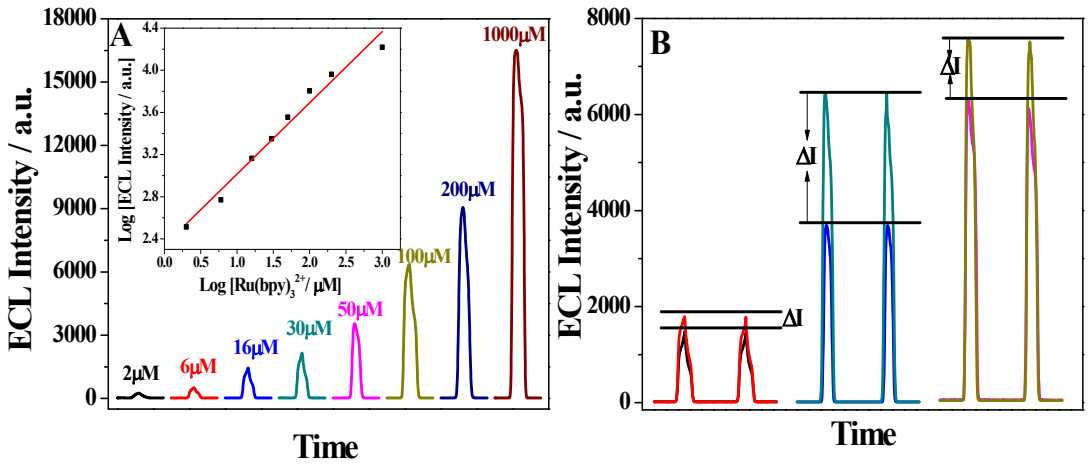

Fig. S8. (A) ECL-potential curves of the B-GQDs/$Ru(bpy)_3^{2+}$ in PBS (pH 9.0) with different $Ru(bpy)_3^{2+}$ concentration, inset: Calibration curve for $Ru(bpy)_3^{2+}$; (B) Effect of $Ru(bpy)_3^{2+}$ concentration on the change of ECL intensity with PCP.

Selectivity, reproducibility and stability of the ECL senseing

Further, the long-term stability of the as-constructed ECL sensor was investigated during 25 days by measuring the ECL response upon of B-GQDs/$Ru(bpy)_3^{2+}$ system in 0.1 M PBS (pH 9.0) with adding 50 pg mL^{-1} PCP (Fig.S9A). In a series of five electrodes prepared in the same way, a relative standard deviation (RSD) of 4.5% was obtained, indicating the reliability of the 25 days.

In addition, the specifity of this ECL sensor was studied using 3-chlorophenol (3-CP), 2,4,6-trichlorophenol (1,3,5-TCP), and 2,4-dichlorophenol (2,4-DCP) as inerferents. As shown in Fig. S9B, only PCP enhanced the ECL emission of B-GQDs/$Ru(bpy)_3^{2+}$ system dramatically, whereas the analogs of PCP changed the ECL emission slightly (e.g., 3-CP, 1,3,5-TCP, 2,4-DCP). The reason might be attributed to that the above interferents possess more stable chemical properties, which did not make a better facilitate effect to electrochemical reaction of $Ru(bpy)_3^{2+}$.

Fig. S9

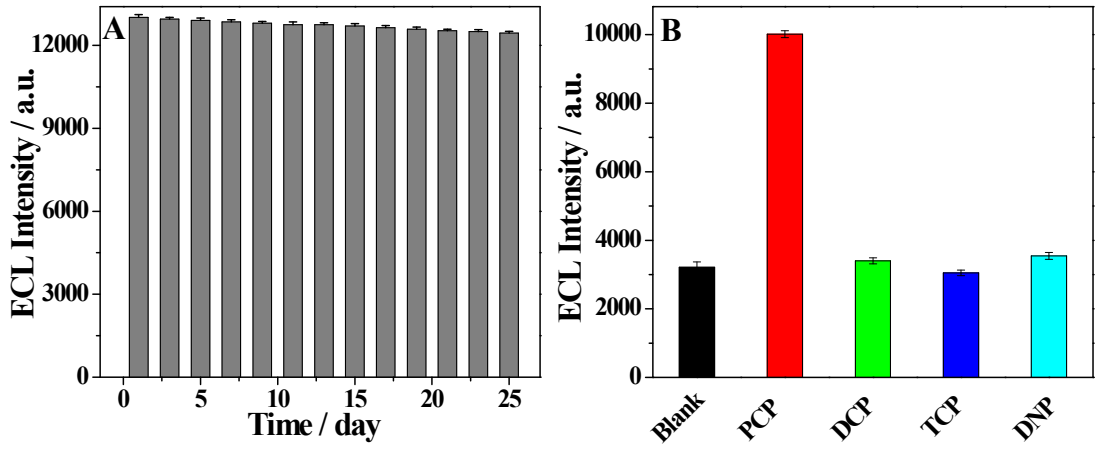

Fig. S9. (A) Stability of the ECL sensor over 25 days in 0.1 mol L^{-1} PBS (pH 9.0) with 50 pg mL^{-1} PCP; (B) ECL of 10 pg mL^{-1} DCP, TCP, DNP and PCP on the responses of the sensor in 0.1 mol L^{-1} PBS (pH 9.0).

Table S2 Comparison of other ECL systems for determination of PCP

Materials	Linear range	Detection limit	Ref.
GQDs-CdS NCs	0.01 ~ 500 ng mL^{-1}	3 pg mL^{-1}	[8]
CuO NWs/rGO	0.027 ~ 266.3 ng mL^{-1}	9 pg mL^{-1}	[9]
MWCNTs@GONRs	0.002 ~ 10 ng mL^{-1}	0.7 pg mL^{-1}	[10]
B-GQDs	0.02 ~ 150 pg mL^{-1}	6.7 fg mL^{-1}	this work

Notes and references

1 D. Y. Pan, J. C. Zhang, Z. Li and M. H. Wu, *Adv. Mater.,* 2010, **22,** 734–738.

2 J. H. Shen, Y. H. Zhu, C. Chen, X. L. Yang and C. Z. Li, *Chem. Commun.,* 2011, **47,** 2580–2582.

3 C. Gomez-Navarro, R. T. Weitz, A. M. Bittner, M. Scolari, A. Mews, M. Burghard and K. Kern, *Nano Lett.,* 2007, **7,** 3499–3503.

4 J. Peng, W. Gao, B. K. Gupta, Z. Liu, R. Romero-Aburto, L. H. Ge, L. Song, L. B. Alemany, X. B. Zhan, G. H. Gao, S. A. Vithayathil, B. A. Kaipparettu, A. A. Marti, T. Hayashi, J. J. Zhu, P. M. Ajayan, S. A. Vithayathil, B. A. Kaipparettu, A. A. Marti, T. Hayashi, J. J. Zhu and P. M. Ajayan, *Nano Lett.,* 2012, **12,** 844−849.

5 K. J. Wei Y., Wang, W. Q. Han, J. S. Li, X. Y. Sun, J. Y. Shen and L. J. Wang, *J. Power Sources,* 2016, **318,** 57−65.

6 P. Han, T. Yuan, L. Yao, Z. Han, J. H. Yang and S. Y. Zheng, *Nanoscale Res. Lett.,* 2016, **11,** 1–8.

7 W. Xie, H. F. Cheng, Z. Y. Chu, Z. H. Chen and C. G. Long, *Ceram. Int.,* 2011, **37,** 1947–1951.

8 Q. Liu, K. Wang, J. Huan, G. B. Zhu, J. Qian, H. P. Mao and J. R. Cai, *Analyst,* 2014, **139,** 2912–2918.

9 W. Q. Wu, X. Hua, S. L. Luo, C. B. Liu, Y. H. Tang and L. M. Yang, *Sens. Actuators B,* 2016, **222,** 747–754.

10 Q. Liu, J. Huan, A. R. Fei, H. P. Mao and K. Wang, *Talanta,* 2015, **134,** 448–452.